



HAL
open science

Abrupt warming and salting of the Western Mediterranean Deep Water: atmospheric forcings and lateral advection.

Katrin Schroeder, S. A. Josey, Marine Herrmann, Laure Grignon, G. P. Gasparini, H. L. Bryden

► **To cite this version:**

Katrin Schroeder, S. A. Josey, Marine Herrmann, Laure Grignon, G. P. Gasparini, et al.. Abrupt warming and salting of the Western Mediterranean Deep Water: atmospheric forcings and lateral advection.. *Journal of Geophysical Research. Oceans*, 2010, 115 (C08029), pp.18. 10.1029/2009JC005749 . insu-00562614

HAL Id: insu-00562614

<https://insu.hal.science/insu-00562614>

Submitted on 5 Mar 2021

HAL is a multi-disciplinary open access archive for the deposit and dissemination of scientific research documents, whether they are published or not. The documents may come from teaching and research institutions in France or abroad, or from public or private research centers.

L'archive ouverte pluridisciplinaire **HAL**, est destinée au dépôt et à la diffusion de documents scientifiques de niveau recherche, publiés ou non, émanant des établissements d'enseignement et de recherche français ou étrangers, des laboratoires publics ou privés.

Abrupt warming and salting of the Western Mediterranean Deep Water after 2005: Atmospheric forcings and lateral advection

K. Schroeder,¹ S. A. Josey,² M. Herrmann,³ L. Grignon,² G. P. Gasparini,¹ and H. L. Bryden²

Received 27 August 2009; revised 2 December 2009; accepted 9 April 2010; published 27 August 2010.

[1] The recent major production of anomalously warm, salty deep water in the northwestern Mediterranean Sea (winters 2004–2005 and 2005–2006) is linked to extreme winter air–sea heat and freshwater forcing of the basin. Fields of heat and density fluxes are determined both from the National Centers for Environmental Prediction–National Center for Atmospheric Research reanalysis and a daily high-resolution downscaling of the European Centre for Medium-Range Weather Forecasts reanalysis and analysis data set ARPERA. In the deep water formation region, during winter 2004–2005, the net heat loss exceeds 300 W m^{-2} compared with typical values of 200 W m^{-2} . The relationship between the deep water formation episodes and large-scale atmospheric patterns is investigated and found to be more closely related to the East Atlantic Pattern than the North Atlantic Oscillation. The contributions of atmospheric forcing and lateral advection of anomalously warm, salty water to the convection region are discussed in order to determine their relative roles in causing massive renewal of Western Mediterranean Deep Water and its anomalous properties. The main result shows that the net evaporation during winter 2004–2005, even if very high compared to the climatology, could have induced only 49% of the actual observed increase in the salt content of the deep layer. Thus, lateral advection played a major role in setting the new deep water properties.

Citation: Schroeder, K., S. A. Josey, M. Herrmann, L. Grignon, G. P. Gasparini, and H. L. Bryden (2010), Abrupt warming and salting of the Western Mediterranean Deep Water after 2005: Atmospheric forcings and lateral advection, *J. Geophys. Res.*, *115*, C08029, doi:10.1029/2009JC005749.

1. Introduction

[2] The northwestern Mediterranean Sea (NW-MED) is a deep-intermediate convection region; thus, it is among the few sites worldwide that are able to redistribute water over great depths. As a consequence, layers which are typically not exposed to the atmosphere may lose heat, which on longer time scales is balanced by convergence of heat into the region, as a result of the general circulation. In general, the combination of surface heat and freshwater losses and the lateral convergence of heat and freshwater sustains the deep convection in this area, as in other convection regions [Straneo, 2006]. In a steady state, one would expect a balance between the removal of heat or freshwater by the atmosphere and the supply of those properties by the adjacent ocean. In particular, in the NW-MED during winter, dry and cold air initially mixes the Atlantic Water (AW)

with the underlying warmer and saltier Levantine Intermediate Water (LIW), and further heat loss leads to the formation of Western Mediterranean Deep Water (WMDW). The AW enters the basin through the Strait of Gibraltar and is gradually transformed along its path through the whole Mediterranean. The LIW is formed in the Levantine sub-basin, from where it spreads westward toward the Sicily Channel and Gibraltar, becoming the bulk of the outflowing Mediterranean water [Millot and Taupier-Letage, 2005]. Dense water formation (DWF) processes are known to occur in the Gulf of Lions [MEDOC Group, 1970], the Catalan subbasin [Salat and Font, 1987], and the Ligurian Sea [Sparnocchia et al., 1995]. The formation of the WMDW depends on a preconditioning period, followed by violent mixing. Finally, the deep water formed spreads out of the convective region [Rhein, 1995].

[3] Recently, a significant warming and salinification of the whole water column has been observed and several studies have revealed the abundant formation of a new warmer and saltier WMDW during winters 2004–2005 and 2005–2006 [Schroeder et al., 2006, 2008a; Font et al., 2007; Smith et al., 2008]. The bulk of the new WMDW, in the abyssal plain of the western Mediterranean Sea (WMED), showed temperatures of 12.85° – 12.88°C and salinities of

¹Istituto di Scienze Marine, CNR, Sede di La Spezia, Forte Santa Teresa, Pozzuolo di Lerici, Italy.

²National Oceanography Centre, Southampton, UK.

³Centre National Recherche Météorologique, Groupe d'études de l'Atmosphère Météorologique, Météo-France, CNRS, Toulouse, France.

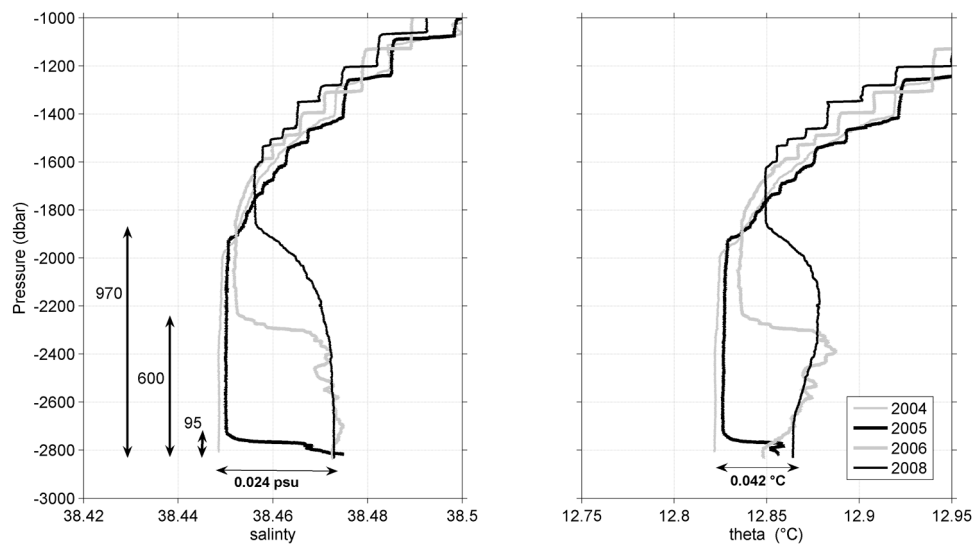


Figure 1. Vertical profiles of (left) salinity and (right) potential temperature measured at an example station in the Algerian basin (5°E , 38°N) in October 2004 (shaded thin), June 2005 (bold line), October 2006 (shaded bold line) and November 2008 (thin line). Vertical arrows indicate the thickness of the new Western Mediterranean Deep Water (WMDW) layer in the different years. Horizontal arrows indicate total salinity and temperature increase at the bottom between 2004 and 2008.

38.455–38.473 below 2000 m depth [Schroeder *et al.*, 2008a]. Between 2004 and 2008 the new WMDW occupied a layer becoming hundreds of meters thick, with total increases of salinity and temperature of about $\Delta S = 0.024$ and $\Delta\theta = 0.042^{\circ}\text{C}$, respectively, near the bottom (see data in Figure 1, station located south of the Balearic Islands at 5°E , 38°N). By October 2008 the new deep water has been found everywhere in the western basin below 2000 m depth, with the exception of the Tyrrhenian subbasin [Schroeder *et al.*, 2009]. Furthermore, it has been uplifted toward the Alboran subbasin, where in 2008 it was detected along the Moroccan continental slope at depths <1000 m. The magnitude of the replacement of the old deep water by the new deep water is well evident in the vertical profiles shown in Figure 1.

[4] The anomaly described above has its origin in new DWF in the NW-MED during two winters: 2004–2005 [Lopez-Jurado *et al.*, 2005; Font *et al.*, 2007; Schroeder *et al.*, 2006] and 2005–2006 [Schroeder *et al.*, 2008a; Smith *et al.*, 2008]. During the severe winter 2004–2005, deep convection occurred mainly in the Gulf of Lions and in the Catalan subbasin. These sites may also have received a higher amount of salt and heat before the onset of convection by lateral advection. Winter 2005–2006 has shown deep convection in the Ligurian Sea [Smith *et al.*, 2008; Schroeder *et al.*, 2008b, Figure 2b]. Schroeder *et al.* [2006] related the new deep properties to a progressive increase of heat and salt content in the intermediate layer, due to the arrival of water of eastern origin, which has been affected by the Eastern Mediterranean Transient (EMT), a major deep water formation event that took place in the eastern Mediterranean Sea (EMED) between the late 1980s and mid 1990s [Roether *et al.*, 2007; Samuel *et al.*, 1999; Josey, 2003]. The EMT has been recognized as a plausible candidate to influence deep water production in the WMED by other authors [Lopez-Jurado *et al.*, 2005; Font *et al.*, 2007]. In both

studies the observed anomalies have also been related to the extremely strong forcings in winter 2004–2005. In terms of air-sea heat exchange, using the National Centers for Environmental Prediction-National Center for Atmospheric Research (NCEP-NCAR) reanalysis, Lopez-Jurado *et al.* [2005] showed that the heat loss of this winter was 70% above the winter average, with the highest values since 1948. Additionally, in terms of air-sea freshwater exchanges, Font *et al.* [2007] assert that in autumn 2004 and winter 2004–2005 precipitation over the NW-MED catchment area was greatly reduced, with the lowest absolute values ever recorded at many of the meteorological stations, and that northerlies were strong and persistent. Hereafter the recent DWF events will be referred to as the Western Mediterranean Transition (WMT), as described by *Commission Internationale pour l'Exploration Scientifique de la mer Méditerranée (CIESM)* [2009].

[5] In this paper, we investigate the causes of the WMT, in particular the abrupt changes in the heat and salt contents of the WMDW, in order to define the relative roles of the atmospheric forcings (air-sea heat and freshwater fluxes) and the advection of anomalously salty and warm water to the convection region. The paper presents for the first time a detailed analysis of the conditions that triggered the recent formation of the new WMDW. In section 2, we describe the data and methods employed for our analysis. Section 3 focuses on the air-sea fluxes of heat and density, which are essential to estimate the lateral advection of these properties within the ocean. Variations in the strength of the air-sea fluxes are investigated using a dynamical downscaling of the European Centre for Medium-Range Weather Forecasts (ECMWF) reanalysis and analysis data set for recent winters, including 2004–2005, and the coarser resolution NCEP-NCAR reanalysis to provide the long-term and large-scale contexts. The interannual and seasonal variability of heat and salt contents of the water column

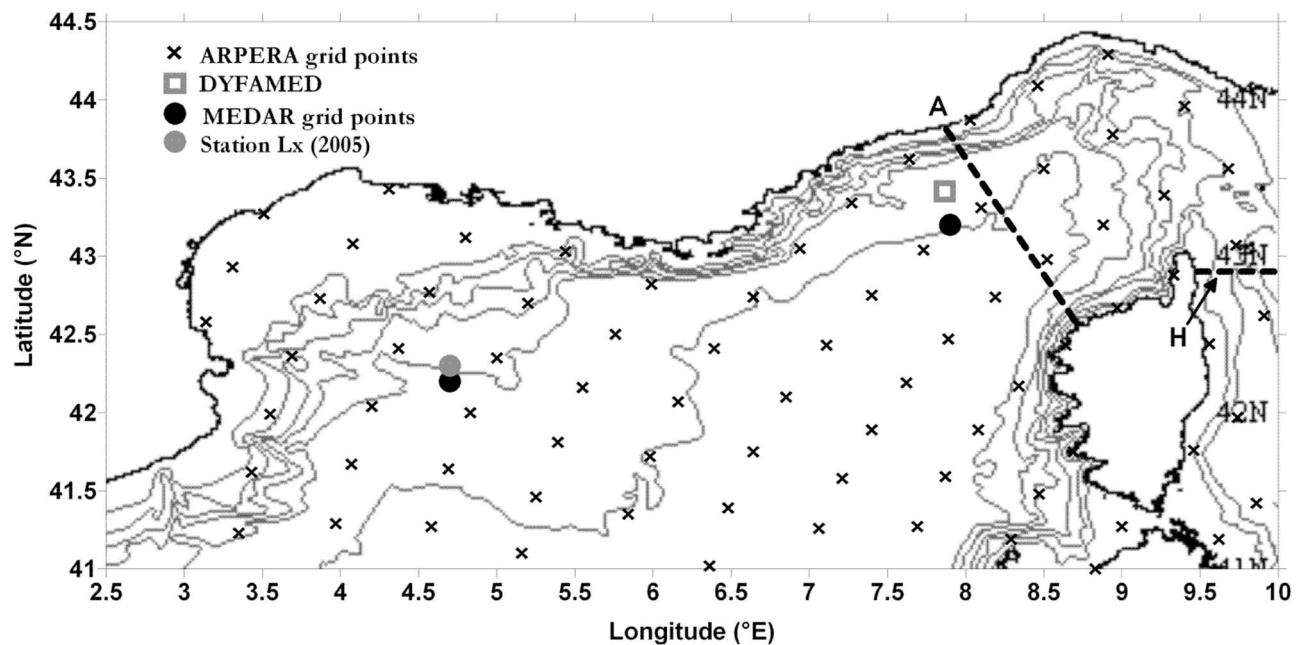


Figure 2. Map of the investigated region in the northwestern Mediterranean. Black crosses indicate ARPERA data set grid points, the shaded square the DYFAMED site, the shaded circle the Lx station (May 2005), and the black circle the MEDAR grid point used for calculations. For clarity, across the Corsica Channel and in the Ligurian Sea, transects A and H described by *Schroeder et al.* [2008c] are shown as dashed bold lines.

is analyzed in section 4 using measurements from the Dynamique des Flux Atmosphériques en Méditerranée (DYFAMED) site (Figure 2). The assumption is that we consider the water properties observed at this site as a “proxy” for the water advected to the convection area. The lateral advection of heat and salt (section 5), computed as the difference between the heat and salt content changes and the surface fluxes, represents “hydrographic” preconditioning of the water column. By this term we refer to the heat and salt content in the water column before the onset of convection, as opposed to “dynamical” preconditioning, which is related to doming of the isopycnals due to cyclonic circulation. Finally, with regard to the different hypotheses mentioned above, section 6 is an attempt to quantify the different contributions (strength of the atmospheric forcings vs. accumulation of heat and salt) setting the anomalous WMDW properties.

2. Data and Methods

2.1. Hydrographic Data

[6] Recently, the Italian National Research Council (CNR) conducted several surveys in the WMED with the R/V *Urania* (see composite map in *Schroeder et al.* [2008a]). For the purpose of this study we have used only a few conductivity-temperature-depth (CTD) stations: a station south of the Balearic Islands, at 5°E, 38°N (location not shown, data in Figure 1), visited in October 2004, June 2005, October 2006, and November 2008 in order to illustrate the temporal evolution of the new deep properties and stratification; and station Lx in the Gulf of Lions visited on 1 May 2005 (Figure 2, shaded filled circle, $z = 1996$ m). Pressure, salinity, potential temperature and dissolved oxygen were measured with a

SBE 911*plus* CTD. The probes were pre- and post-calibrated at the NATO Undersea Research Centre in La Spezia (Italy). During the cruise, CTD salinity measurements were checked against samples analysed with a Guildline Autosal salinometer.

[7] CTD data collected almost every month by the Observatoire Océanologique de Villefranche sur Mer Service d’Observation (<http://www.obs-vlfr.fr/sodydf/>) at the DYFAMED site (Figure 2, shaded empty square, $z = 2000$ m), were used to observe the temporal evolution of heat and salt contents in the Ligurian Sea, for the period 1995–2008.

[8] Finally, we used data from two grid points in the Mediterranean Data Archaeology and Rescue (MEDAR) (<http://www.ifremer.fr/sismer/program/medar/>) MEDATLAS II climatology database [*MEDAR Group*, 2002]. This climatological data set was produced from observations that were quality controlled and interpolated onto a regular spatial grid. The processing is described at <http://www.ifremer.fr/medar/climatol.htm>. Climatological data (only annual values are available), which we use here, can be downloaded for the whole Mediterranean, with vertical resolutions of 5 m near the surface to 500 m at the bottom. We have used the 2002 annual average profiles of temperature and salinity in the Gulf of Lions at 42.2°N, 4.7°E and in the Ligurian Sea at 43.2°N, 7.9°E (Figure 2, black filled circles, for both grid points $z = 2000$ m).

2.2. Air-Sea Fluxes

[9] For the air-sea flux analysis we use the ARPERA data set, presented by *Herrmann and Somot* [2008], obtained by applying dynamical downscaling based on spectral nudging to a low-resolution data set. The principle is to use a high-resolution atmospheric model in which small scales can

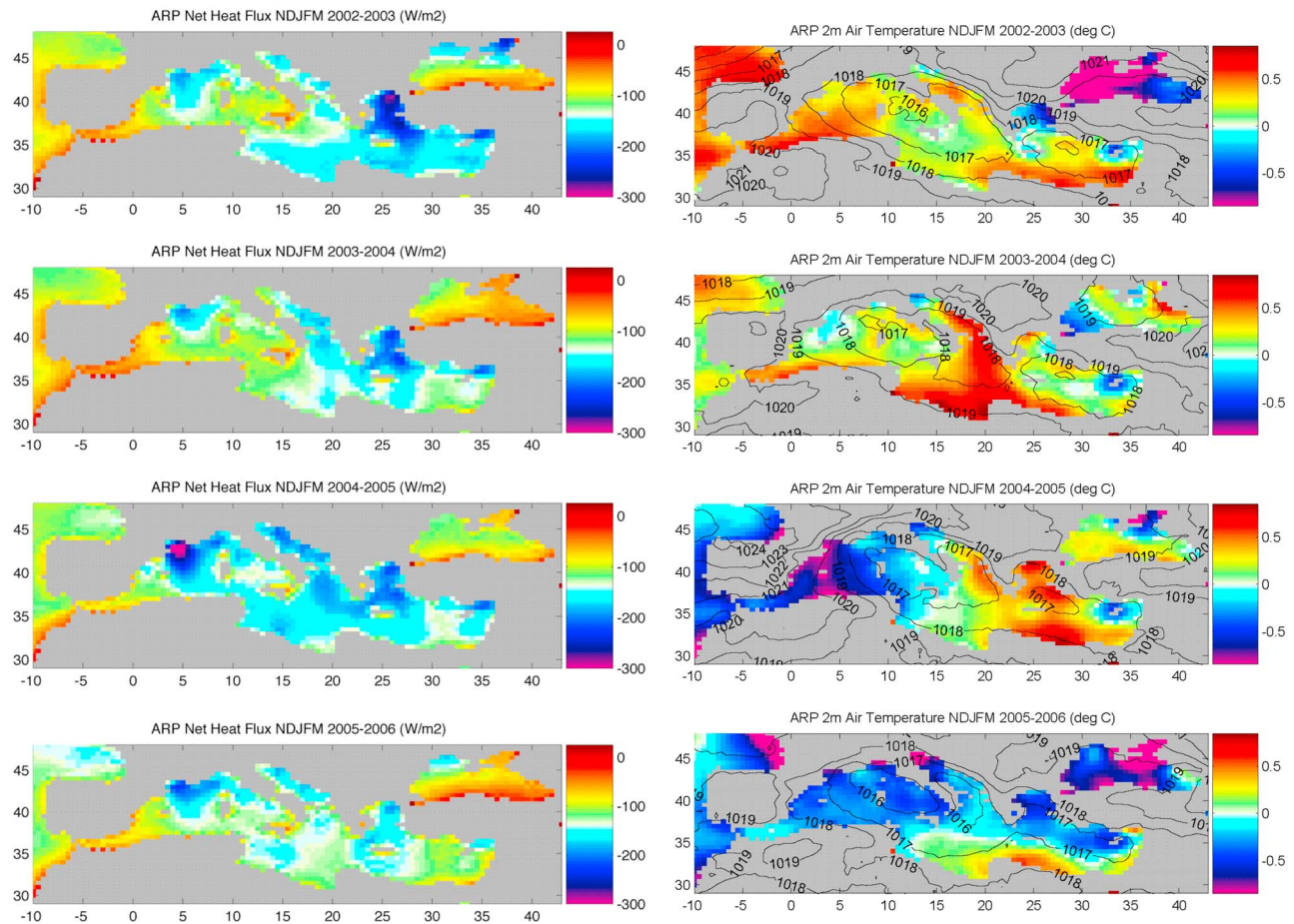


Figure 3. For each of the four winters from 2002–2003 to 2005–2006 (left) net air-sea heat flux from the ARPERA data set (negative values represent heat loss from the ocean to the atmosphere) and (right) fields of 2 m air temperature anomalies (colour) and sea level pressures (contours) from the ARPERA data set.

develop freely and large scales are driven by the lower resolution data set. The synoptic chronology then follows that of the low-resolution data set while the high resolution structures of the atmospheric flow are created by the model. A stretched grid version of the Atmosphere General Circulation Model, ARPEGE-Climate [Déqué and Piedelievre, 1995], of about 50 km resolution in the Mediterranean region, was used to perform this downscaling. The limit of the waves driven by the low-resolution data set was 250 km, and a nudging term was added to the equations of the temporal evolution of the prognostic variables (temperature, velocity, and surface pressure). From coupled simulations at different resolutions, Li *et al.* [2006] and Herrmann and Somot [2008] concluded that the necessary atmospheric resolution in order to simulate the Mediterranean convection and DWF is about 50 km. The ARPEGE project initially considered the period 1958–2001, which coincided with the time frame of the ECMWF 40 year reanalysis (ERA40) [Simmons and Gibson, 2000]. For this period, the 125 km resolution reanalysis fields were downscaled to 50 km. Subsequently, the ARPEGE project was extended to cover the period 2002–2006. However, reanalysis fields were not available for 2002–2006, so it was necessary to use the analysis (also termed operational) fields from ECMWF for

this period. These are already available on a 50 km grid, so to ensure consistency with the earlier period it was necessary to first degrade them to the same resolution (125 km) employed previously. It would have been preferable to use ECMWF fields at the same resolution for the entire period considered (1958–2006); however, this has not been possible given the lack of availability of ECMWF reanalysis data beyond the end of 2002. Hence, we have taken the approach described above.

[10] In addition to ARPERA, we employ the NCEP-NCAR reanalysis [Kistler *et al.*, 2001] to place the extreme winter 2004–2005 forcing of the WMED in a large-scale context and relate it to the major modes of atmospheric variability over the Atlantic Ocean. We use NCEP as a consistency check to test whether similar results are obtained using a reanalysis with a different atmospheric model to that employed for ECMWF.

3. Air-Sea Fluxes

3.1. Surface Heat Fluxes

[11] The net air-sea heat flux from the ARPERA data set for each of the four winters from 2002–2003 to 2005–2006 is shown in Figure 3 (left). Here, winter is defined as the

Table 1. Mean Net Heat Flux and Components for the Box (42° – 43° N, 4° – 5° E) for the Extreme Winter 2004–2005 and the Average of the Three Other Winters Considered (2002–2003, 2003–2004, and 2005–2006), from the ARPERA data set

	2004–2005	Other Winters
Net (W m^{-2})	–308	–201
Latent (W m^{-2})	–243	–171
Sensible (W m^{-2})	–81	–47
Longwave (W m^{-2})	–84	–77
Shortwave (W m^{-2})	100	94

period November–March, in order to include all months likely to have a direct impact on deep convection (alternative winter definitions, e.g., Dec–Feb, have been considered and produced similar results). As expected, winter 2004–2005 stands out as having extreme surface forcing in the Gulf of Lions region. The typical winter mean heat loss in this region is around 200 W m^{-2} , while an extremely high winter mean of 300 W m^{-2} was observed in winter 2004–2005. This is revealed more clearly in Table 1 which contains the winter mean net heat flux and its components for a four grid cell box (42° – 43° N, 4° – 5° E) centered on the region of most extreme heat loss. The wintertime mean heat flux for 2004–2005 is -308 W m^{-2} , more than 100 W m^{-2} stronger than the mean loss of -201 W m^{-2} for the other three winters considered. Most of the additional heat loss is

due to an increase in the latent heat loss by 72 W m^{-2} while the sensible heat loss contributes an extra 34 W m^{-2} . The two radiative terms show small changes of 6 – 7 W m^{-2} cancelling each other out; thus, they have no net impact on the enhanced heat loss.

[12] The month to month variation between January 2002 and December 2007 is seen more clearly in Figure 4 which shows time series of the net heat flux and its components averaged over the same area (42° – 43° N, 4° – 5° E). In contrast to the other winters in this period, winter 2004–2005 has a prolonged period of four months (November–February) with extremely strong heat loss resulting in the large negative values seen in Table 1. Table 1 and Figure 4 confirm that the dominant term in the winter 2004–2005 surface fluxes is the latent heat flux, which peaks with a value of -290 W m^{-2} in February 2005. The sensible heat flux also plays an important role, falling below -100 W m^{-2} in February 2005 as the only occasion in the time series. As noted for the box mean above, the two radiative terms (shortwave and longwave) show little variation from their typical values in winter 2004–2005. Thus, this winter is seen to be one of extreme ocean heat loss to the atmosphere as a result of combined turbulent (sensible and latent) heat loss.

[13] The driving meteorological terms for the strong 2004–2005 surface heat loss are now considered. Figure 3 (right) shows the mean sea level pressure field and anomalous 2 m air temperature pattern (where anomalies are

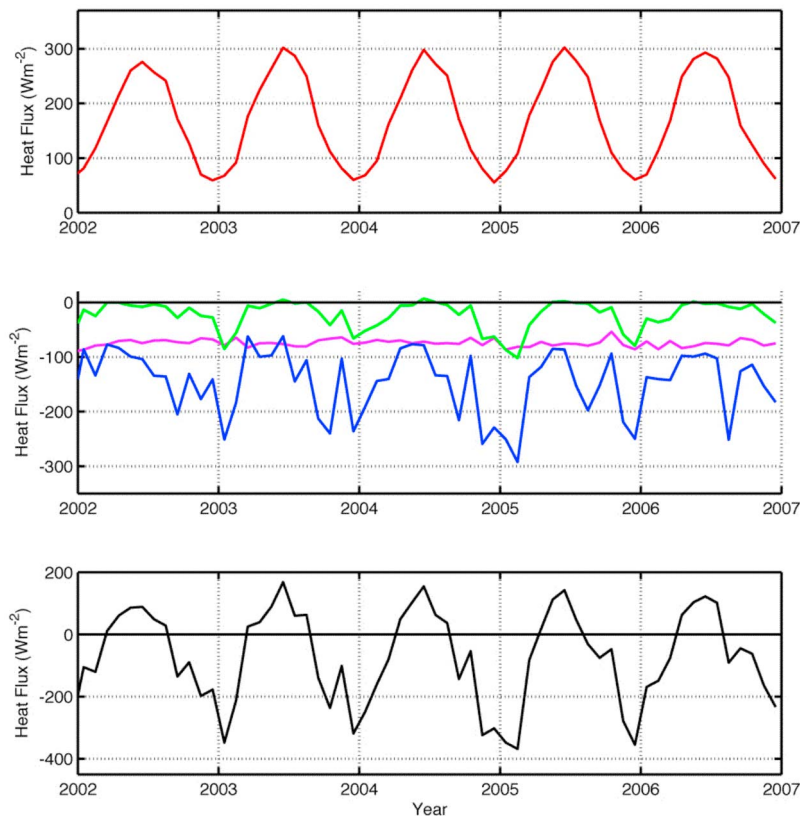


Figure 4. Time series from the ARPERA data set of the net heat flux and its components, averaged over grid cells in the the box (42° – 43° N, 4° – 5° E), centered on the region of most extreme heat loss. Red, shortwave; magenta, longwave; green, sensible; blue, latent; and black, net heat fluxes.

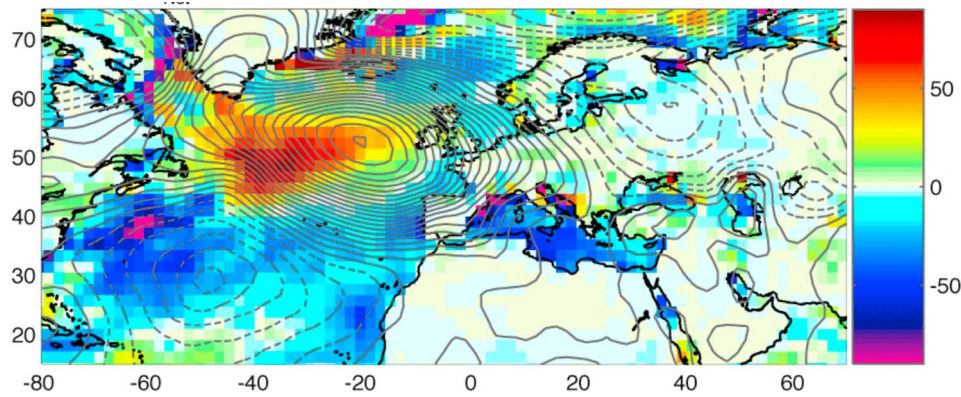


Figure 5. Large-scale surface pressure field (contours at 0.5 mbar intervals, positive values solid) and net heat flux anomaly (colored field, units W m^{-2}) for winter 2004–2005 from the the National Centers for Environmental Prediction–National Center for Atmospheric Research (NCEP–NCAR) reanalysis.

determined with respect to the full period spanned by the model run, i.e. 1958–2006) for each of the four winters. The 2004–2005 field has a much stronger east–west pressure gradient in the WMED than the other three winters, with an associated intense northerly flow over the Gulf of Lions revealed by the closely spaced isobars. This gives rise to winter mean air temperature anomalies up to 1°C colder than the mean over the deep convection region. The reduction in air temperature combined with the strong northerly winds leads to the greater heat loss noted above.

[14] We now investigate how surface forcing for 2002–2006 relates to the larger horizontal scales, in order to determine the influence of atmospheric variability over the Atlantic. For this, we employ the NCEP–NCAR reanalysis. The large-scale surface pressure field (contours at 0.5 mbar intervals, positive values solid) and net heat flux anomaly for winter 2004–2005 is shown in Figure 5. Strong heat loss in the Gulf of Lions convection region is associated with advection of cold dry air from the European land mass. Thus, despite their coarser resolution, the NCEP fields provide a picture consistent with the finer resolution ARPERA analysis. Furthermore, this indicates a consistent driving mechanism for the observed deep convection between both the NCEP and ECMWF reanalyses.

[15] The sea level pressure fields over the Atlantic exhibits a structure with anomalously high pressure, up to 10 mbar greater than the long term mean, centered on 53°N , 20°W , and a much weaker low pressure anomaly, 3 mbar less than the mean, centered on 30°N , 50°W . The leading modes of atmospheric variability over the North Atlantic have been discussed in various studies [e.g., Rogers, 1990; Josey *et al.*, 2001; Josey and Marsh, 2005], with the first and second modes being the North Atlantic Oscillation (NAO) and the East Atlantic Pattern (EAP), respectively. The anomaly field shown in Figure 5 cannot be clearly identified with either mode. However, it more closely resembles the negative phase of the EAP, which is characterized by a dominant high pressure anomaly to the west of Ireland, as opposed to the NAO which has a north–south dipole with centers of action over the Azores and Iceland. This result is supported by an analysis of indices for each of these modes during winter 2004–2005 obtained from the NOAA/National

Weather Service Climate Prediction Center. For this period the EAP index = -0.61 while the NAO index = 0.31 .

3.2. Surface Density Flux

[16] The net heat flux and the net evaporation can be combined to obtain the density flux (F_ρ) into the ocean surface [Gill, 1982; Schmitt *et al.*, 1989; Josey, 2003], which is the sum of the thermal (F_T) and haline (F_S) contributions

$$F_\rho = -\rho \left(\alpha \frac{Q_{\text{NET}}}{\rho c_p} - \beta S \frac{E - P}{(1 - S/1000)} \right) = F_T + F_S = \frac{B}{g}, \quad (1)$$

where ρ is the density of water at the sea surface, c_p is the specific heat capacity of water, and S is the sea surface salinity. The terms α and β are the thermal expansion and haline contraction coefficients, respectively. Values for the salinity have been obtained by the monthly MEDAR climatology [MEDAR Group, 2002]. The terms Q_{NET} and $E - P$ are taken from ARPERA. Heat loss from the ocean to the atmosphere ($Q_{\text{NET}} < 0$) and net evaporation ($E > P$) results in positive values of F_ρ , F_T , and F_S , which means that the density of the near surface layers increases. The density flux is related to the buoyancy flux B by the acceleration due to gravity ($g = -9.8 \text{ m s}^{-2}$), so that an increase in density of the ocean surface corresponds to buoyancy loss. Figure 6 shows the daily density flux during the winters of 2004–2005 (at the ARPERA grid point in the Gulf of Lions, 4.83°E , 42°N) and 2005–2006 (at the ARPERA grid point in the Ligurian Sea, 8.1°E , 43.31°N), distinguishing between the thermal and haline contributions to the total density flux. In winter 2004–2005, there were at least four strong events with the density flux exceeding $4 \times 10^{-5} \text{ kg m}^{-2} \text{ s}^{-1}$, while during winter 2005–2006, there were only two events that reached the same threshold. In both winters, the net evaporation, proportional to F_S , has a much weaker impact on the total density flux than F_T , related to heat loss. This suggests that the greatly reduced precipitation in fall 2004, argued by Font *et al.* [2007] as a possible cause of the WMT, did not play an important role in the intensity of the convection. It is worth noting that small variations of the sea surface salinity (of about 0.2, as may be observed during the winter and which perhaps is not well represented in the monthly mean

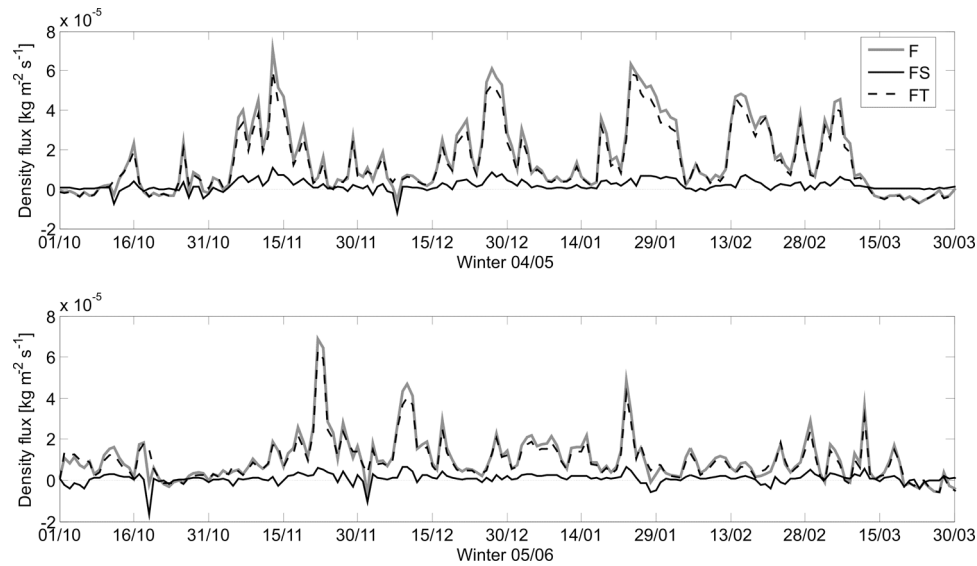


Figure 6. Daily density fluxes during the two winters 2004–2005 (at the ARPERA grid point in the Gulf of Lions, 4.83°E, 42°N) and 2005–2006 (at the ARPERA grid point in the Ligurian Sea, 8.1°E, 43.31°N).

values of the MEDAR climatology) would induce a variation of the resulting F_S less than 0.5%, thus not affecting significantly the results shown in Figure 6.

4. Heat and Salt Contents of the Water Column

[17] In this section, the variations in the heat and salt contents at the DYFAMED site are presented. Since the main goal is to quantify the importance of lateral fluxes in setting the properties of the new WMDW, a fundamental step is the assessment of the heat and salt contents of the whole water column before and after the DWF events. We must point out that the heat content is to be intended as internal energy of the water column. To compute the total heat and salt contents of the water column, the following formulas will be used, considering each profile as representative for a unit area:

$$HC = \int_{z=0}^H \rho(z)c_p(z)\theta(z)Adz \quad (2)$$

$$SC = \int_{z=0}^H \rho(z)S(z)Adz, \quad (3)$$

where A is the unit area, H is the depth of the water column, c_p is the specific heat capacity of water, and ρ is the potential density.

[18] The integrated heat and salt content variations are shown in Figures 7a and 7b. To show in detail their temporal evolution, the water column has been decomposed in 10 layers of 200 m thickness, from the surface to 2000 m depth (i.e., the plots show the integration between the two depths defining each layer). The seasonal variability is greater than the interannual variability only in the surface layer (0–200 m). Changes in the deep layers reflect longer-

term trends [Vargas-Yanez *et al.*, 2009] that can be attributed to the history of convection. We used data at the DYFAMED site, which is not exactly located in the convection region, because here the time series from 1995 to 2008 is available. They represent a good indication of what is advected toward the convection region. The figures show also the “convection period” from December to March. Overall, there is a substantial warming and salting signal in each layer, although the signals are not monotonic. The first 400 m have an oscillating pattern throughout the years, but with a marked salinity increase between 2003 and 2006 in the 0–200 m layer. The highest salt content in the surface layer, recorded in summer 2006, was triggered by the strong freshwater loss during winter 2005–2006 in the Ligurian Sea. Generally, during winter this layer (0–200 m) experiences a strong increase in salt content associated to a cooling. The cooling signal between December and March may extend down to 1200 m, as was the case during the strong DWF event of winter 2005–2006. During this event, at these depths the cooling was accompanied by a freshening, instead of an increase in salinity, suggesting that the layers between 200 and 1200 m may have transferred high amounts of heat and salt to the deep layers (1400–2000 m), which abruptly reached the highest heat and salt contents of the whole time series. The intermediate layers (400–1000 m) are characterized by a clearly evident increasing trend, reaching the maximum heat and salt contents in 2004, just before the beginning of the WMT in winters 2004–2005 and 2005–2006. After these two convective winters a strong decrease, both in temperature and salinity, is evident in the intermediate layer, in accordance with the export of salt and heat from this layer to the deep water. This evolution was accompanied by a significant upward displacement of isopycnals at all levels (the relative contribution of changes on isopycnal surfaces and vertical displacement of isopycnals, according to Bindoff and McDougall [1994], will be evaluated in a second paper). The intermediate water has started regaining heat and salt during the last months of the time

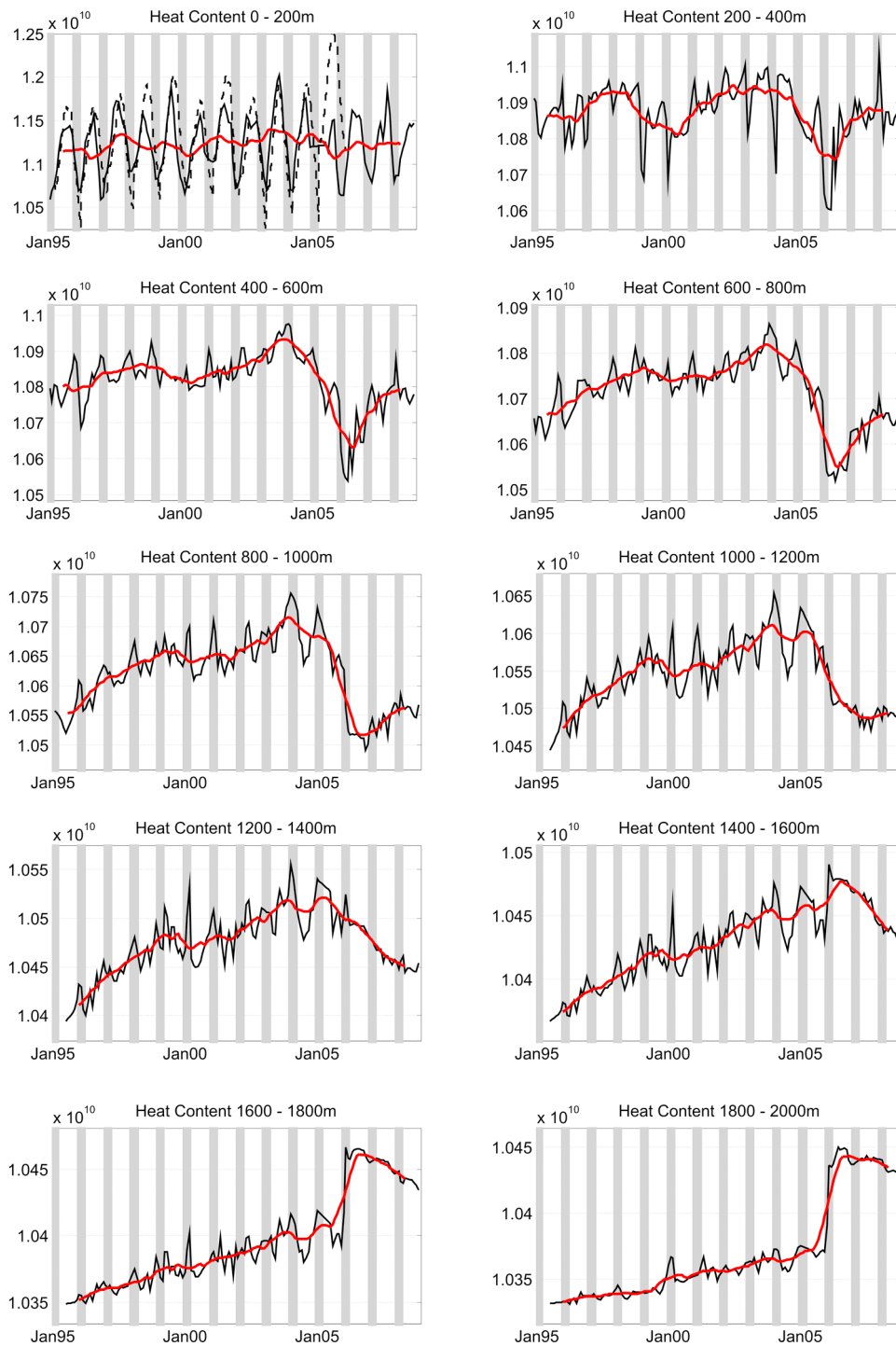


Figure 7. (a) Temporal evolution of heat content (J m^{-2}) at the Dynamique des Flux Atmosphériques en Méditerranée (DYFAMED) site in each 200 m layer from 0 to 2000 m (black line, observed; red line, moving average over 13 months). Shaded regions indicate the “convection period” (December–March). The first plot (0–200 m) shows also the estimated heat content change from the surface fluxes (dashed line). Note that the y -axis scales are different. To obtain approximate corresponding temperature changes, values should be divided by $z c_p \rho \approx 200 \text{ m} \times 4160 \text{ J kg}^{-1} \text{ }^\circ\text{C}^{-1} \times 1029 \text{ kg m}^{-3}$. (b) Same as Figure 7a), except for salt content (10^3 kg m^{-2}). The first plot (0–200 m) shows also the estimated salt content change from the surface fluxes (dashed line). Note that the y -axis scales are different. To obtain approximate corresponding salinity changes, values should be divided by $z \rho \approx 200 \text{ m} \times 1029 \text{ kg m}^{-3}$.

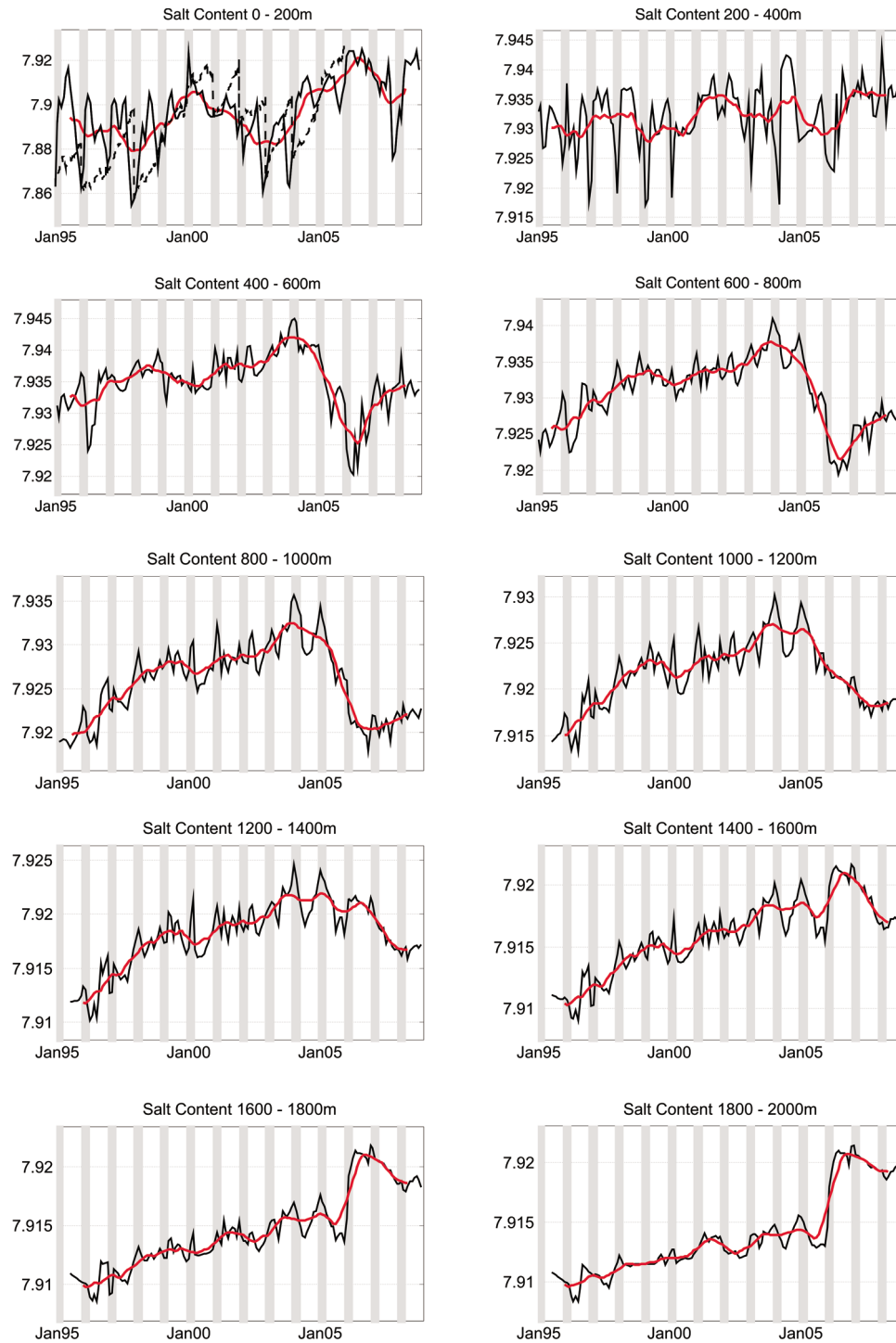


Figure 7. (continued)

series. Between 1000 and 1600 m there is an intermediate/deep transition zone. On the long-term, the deep layers between 1600 and 2000 m show an increasing trend in both properties similar as the intermediate layers, but after the DWF that took place in the Ligurian Sea in February 2006 there is an abrupt jump toward very high salt and heat contents.

[19] This opposite behavior suggests that an internal salt and heat redistribution between the intermediate and the deep layers has occurred during the DWF events. The new deep water is therefore likely to have gained its anomalously high salinity and temperature mainly from the intermediate layer, which during the preceding years has been accumu-

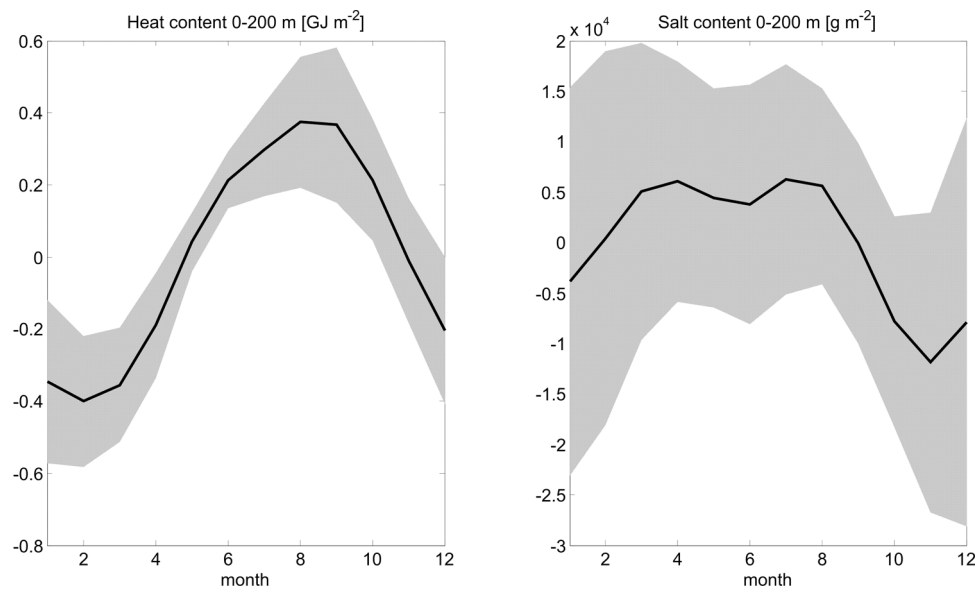


Figure 8. Seasonal variations in heat and salt content anomalies in the surface layer. Shading around the curves indicates the standard deviation.

lating heat and salt, coming from the eastern basin. This issue will be further investigated in section 6.

[20] The mean seasonal cycle in the surface layer (0–200 m), with respect to the annual mean (computed over the whole period of the time series), is shown for both properties in Figure 8. Some important features can be inferred from this figure. For the heat content, the sinusoidal character of the surface forcing dominates. There is a restratification period (April–September) characterized by a warming of the surface layer. The salt content increases from November to March because of the strong evaporation induced by cold and dry winds (Mistral and Tramontane) blowing in this region. The salt content is almost constant during the summer months, with a marked freshening between September and November, probably induced by increased precipitations during fall months. Between September and March, the surface layer undergoes a significant cooling, that may trigger the convection in some years, when combined with the contribution of the increase in salt content in November–March.

5. Lateral Heat and Salt Advection

[21] *Schroeder et al.* [2008c] estimated the transports across different transects in the WMED, using data of spring 2005. To estimate the lateral advection that may affect the convection region, we considered the mass transports from the Tyrrhenian Sea to the Ligurian Sea and from here toward the Gulf of Lions [*Millot and Taupier-Letage, 2005, Figure 3*], and computed the corresponding salt and heat transports. This flow, known as the Northern Current [*Alberola et al., 1995*], moves cyclonically along the coast. Table 2 shows the mass, heat, and salt transports from south to north (between the Tyrrhenian Sea and the Ligurian Sea) and from east to west (between the Ligurian Sea and the Gulf of Lions), and is intended to give insights on the order of magnitude of those transports, distinguishing between surface, intermediate, and deep layer contributions (for reference see *Schroeder et al.* [2008c], their transects A and H are shown also in

Figure 2, for clarity). Their criterion to distinguish the three layers was based on isopycnals (AW between surface and $\sigma_0 = 28.6$; LIW between $\sigma_0 = 28.6$ and $\sigma_{1000} = 33.465$; WMDW between $\sigma_{1000} = 33.465$ and the bottom). A total amount of $85 \times 10^6 \text{ kg s}^{-1}$ of salt and 0.12 PW of heat is advected westward along with the boundary current toward the convection region in the Gulf of Lions. A contribution of about 63% comes from the Tyrrhenian Sea, while the rest is brought by the Corsican Current, on the western side of the Island of Corsica (see Table 2). Overall, the main contributions to the westward lateral advection of heat and salt is due to the surface and intermediate layers. Those transports may not be constant over time. They are largely affected by seasonal and interannual variability of the flow through the Corsica Channel. *Gasparini et al.* [2008], using data from a mooring deployed in the Corsica Channel since 1985, observed that the exchanges between the Tyrrhenian Sea and the Ligurian Sea are particularly sensitive to the imbalance of the winter air–sea exchanges, which may be significantly different in the two subbasins (as reported in Figure 3, left). They also showed that the current, flowing almost permanently from the Tyrrhenian to the Ligurian Sea,

Table 2. Mass, Heat, and Salt Transports Between the Tyrrhenian and Ligurian Seas and From the Ligurian Sea Toward the Gulf of Lions, as Estimated by *Schroeder et al.* [2008c]

	Mass (Sv)	Heat (PW)	Salt (10^6 kg s^{-1})
<i>Between Tyrrhenian and Ligurian Seas</i>			
Surface layer	1.05	0.060	42
Intermediate layer	0.35	0.015	11
Total	1.40	0.075	53
<i>From Ligurian Sea to Gulf of Lions</i>			
Surface layer	1.29	0.067	47
Intermediate layer	0.86	0.047	34
Deep layer	0.20	0.006	4
Total	2.35	0.12	85

has a clear seasonal cycle, with high values in winter and almost negligible values in summer. In addition, the heat and salt transports shown in Table 2 are likely to vary because of the variability of the salt and heat contents of the water volumes transported.

[22] The heat and salt content variations shown in Figure 7 are the result of a combination of heat and freshwater exchanges with the atmosphere (surface fluxes) and the lateral advection from the surrounding ocean (lateral fluxes) and vertical mixing between layers. It is assumed that the latter is negligible except during convection. To what extent changes in the surface layer can be attributed to surface fluxes alone? The previous section already pointed out the predominant seasonality of the surface heat content due to surface fluxes. The question is addressed also by *Grignon et al.* [2010], focusing on the years before 2004–2005, who studied the relative importance of the variability of the surface forcing and preconditioning on the composition of the water formed. In order to assess the importance of the atmospheric forcings, the estimated surface layer heat and salt content changes, derived from ARPERA (section 3.1), are shown for the 0–200 m layer in Figures 7a and 7b (dashed lines). These estimates have been obtained applying (for each year) the ARPERA surface fluxes of ARPERA grid point 8.1°E, 43.31°N (the closest one to the DYFAMED station) to the first 200 m of the water column. With regard to salt, since mass should be conserved, the addition of freshwater to the water column must be accompanied by the removal of the same amount of seawater from the water column. Similarly, the removal of a certain amount of freshwater, due to evaporation, must be accompanied by the replacement of the same amount of water by adjacent seawater, which results in a net addition of salt to the water column. Therefore, the surface salt flux (SSF, in kg m⁻²) is obtained from the surface freshwater flux (SFF = evaporation – precipitation, in m), using

$$\text{SSF} = \text{SFF} \times S_{\text{mean}} \times \rho_0, \quad (4)$$

where S_{mean} is the mean salinity of the water column (between 0 and 200 m) and ρ_0 is the density of freshwater.

[23] It is assumed that, during the restratification period (from April to October), the surface fluxes are acting on the surface layer alone. For both properties, the surface fluxes agree with the observed heat and salt content changes in the surface layer. From the time series shown in Figures 7a and 7b, we calculated that at the DYFAMED site the annual mean net heat loss is $-0.60 \pm 0.53 \times 10^9 \text{ J m}^{-2}$ and that the annual surface freshwater loss induces a mean salt gain of $20.35 \pm 5.40 \text{ kg m}^{-2}$.

[24] The lateral fluxes (lateral heat flux, LHF, and lateral salt flux, LSF) over the total water column are estimated by subtracting the integrated ARPERA surface fluxes (surface heat flux, SHF, and surface salt flux, SSF) from the observed heat and salt content changes (ΔHC and ΔSC):

$$\text{LHF} = \Delta\text{HC} - \text{SHF} \quad (5)$$

$$\text{LSF} = \Delta\text{SC} - \text{SSF}. \quad (6)$$

[25] Using (4) to (6), for the whole time series we estimated annual mean lateral fluxes of $0.70 \pm 0.52 \times 10^9 \text{ J m}^{-2}$

for heat, and $26.98 \pm 23.65 \text{ kg m}^{-2}$ for salt. It is worth noting that the estimated lateral fluxes and the surface fluxes are of the same order of magnitude, for both properties.

[26] In addition to estimating the long-term lateral heat and salt fluxes, this calculation also justifies the use of the ARPERA fluxes for the estimation of the respective roles of surface and lateral fluxes in setting the new WMDW properties, which is discussed in the following section.

6. Impact of Surface and Lateral Fluxes on the New WMDW Properties in Winter 2004–2005

[27] In this section, we try to assess the relative importance of the atmospheric forcings during winter 2004–2005 and the lateral advection of more salt and heat to the convection region, in setting the properties of the new WMDW. *Schroeder et al.* [2008a] suggested that if the exceptionally severe conditions of winter 2004–2005 were responsible for the huge deep water production, as pointed out also by *Lopez-Jurado et al.* [2005], its anomalous characteristics may be due to the progressive heat and salt accumulation in the intermediate layer during the previous years. Under that assumption, the presence of warmer water would need stronger heat fluxes at the sea surface to finally sink and contribute to the deep water formation, but the presence of saltier water would require less heat to be removed to reach a density high enough for sinking to great depths.

[28] As we have reported in the previous sections, winter 2004–2005 showed the strongest heat loss and net evaporation since 1948. But, could these exceptional conditions have produced the warm and salty new deep water? If they had acted onto a climatological water column in the Gulf of Lions, what would have been the resulting heat and salt content? As a “climatological” water column, we chose the θ/S profile of the MEDAR/MEDATLAS climatology [*MEDAR Group*, 2002], corresponding to the annual mean of 2002 at 42.2°N, 4.7°E (Figure 2), with a depth of 2000 m. This point was selected in order to compare it with real CTD data for 1 May 2005 at 42.3°N, 4.7°E (depth 1996 m). In the following computations, we thus compare a hypothetical pre-winter profile (the MEDAR climatological profile, supposed to be on place at the beginning of October 2004, before the onset of strong heat and freshwater losses) with a postwinter profile in the same location (Figure 9a).

6.1. Heat and Salt Contents

[29] First of all, we computed the heat and salt contents of the climatological water column (assumed to be the pre-winter condition) and of the water column after the winter convective event, using (2) and (3). Dividing by H (see section 2.1), gives an estimate of the average heat and salt content per unit of volume ($\langle\text{HC}\rangle$ and $\langle\text{SC}\rangle$). Table 3 shows the total and vertically averaged heat contents (in J m^{-2} and J m^{-3} , respectively) and the total and vertically averaged salt contents (in kg m^{-2} and kg m^{-3} , respectively) for both profiles. The last column indicates the differences between before and after convection: there is a total heat loss of $-6.24 \times 10^8 \text{ J m}^{-2}$ and a total salt gain of 66.3 kg m^{-2} for the whole water column, which means that on average each m^3 along the water column has experienced a heat loss of $-0.03 \times 10^7 \text{ J m}^{-3}$ and a salt gain of $33 \times 10^{-3} \text{ kg m}^{-3}$.

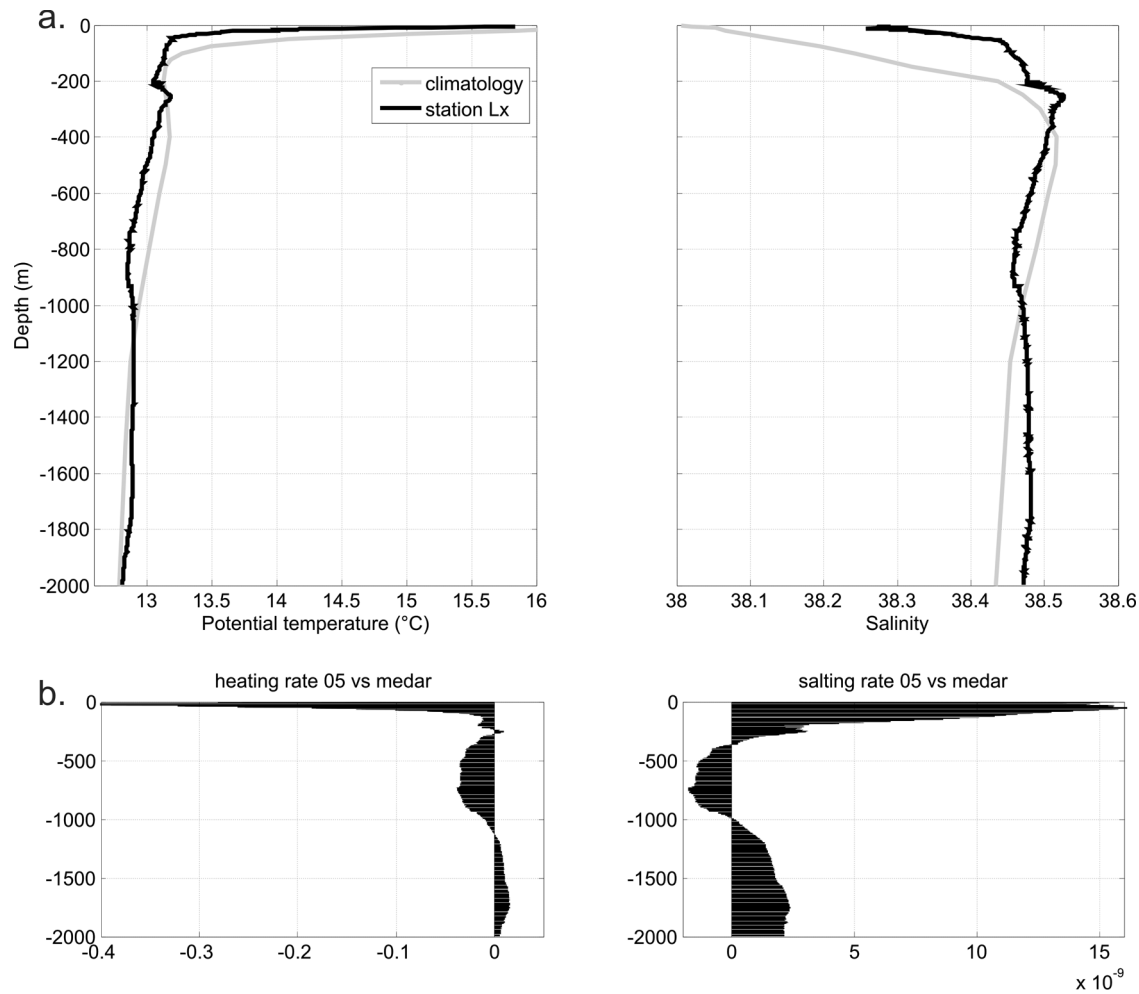


Figure 9. (a) Vertical θ and S profiles of the MEDAR climatology and station Lx; (b) the corresponding vertical distribution of heat (W m^{-3}) and salt ($\text{kg m}^{-3} \text{s}^{-1}$) content changes between the two profiles.

[30] The associated temperature and salinity changes between the pre- and postwinter profiles can be estimated in terms of the heat and salt flux divergence required to produce the observed changes [see *Klink*, 1998]. At each depth we computed thus the heating and the salting rates (Q in W m^{-3} and R in $\text{kg m}^{-3} \text{s}^{-1}$, respectively):

$$Q = \frac{\rho C_P \Delta \theta}{\Delta t} \quad (7)$$

$$R = \frac{\rho \Delta S}{\Delta t}, \quad (8)$$

considering the time interval (Δt , in seconds) from 1 October 2004 to 1 May 2005. In the absence of any lateral advection, the vertical integral of the flux divergences would be equivalent to the net heat or salt flux over a water column with an area of 1 m^2 and extending over the depth range considered for integration (i.e., they are the net surface flux required to produce the observed changes). Figure 9b shows the vertical distribution of the heat and salt changes observed after winter 2004–2005 with respect to the climatological profile, which we are assuming to have been in place before the winter. There is a surface

layer, extending to a depth of about 360 m, characterized by a strong salting and cooling, a pattern that would be expected after such an exceptional winter. The intermediate layer, instead, shows a freshening and a cooling, which might be due to the removal of heat and salt during the convection, and their transfer to the newly formed deep water. Actually, below about 1000 m depth, the vertical distribution of heat and salt changes evidences a salting and a warming of the deep layer, in accordance with the observations described by *Schroeder et al.* [2006, 2008a], *Lopez-Jurado et al.* [2005], and *Font et al.* [2007].

Table 3. Heat and Salt Contents of Two Profiles and Their Differences

Gulf of Lions	MEDAR Station ^a (Prewinter)	Lx Station (Postwinter)	Δ
HC (J m^{-2})	$1.0560 \pm 3.13 \times 10^{11}$	1.0498×10^{11}	-6.24×10^8
SC (kg m^{-2})	$7.8926 \pm 2.19 \times 10^4$	7.8992×10^4	66.3
<HC> (J m^{-3})	$5.28 \pm 0.0015 \times 10^7$	5.25×10^7	-0.03×10^7
<SC> (kg m^{-3})	39.562 ± 0.011	39.595	33×10^{-3}

^aMEDAR profile values include errors which were computed after taking into account the temperature and salinity error fields.

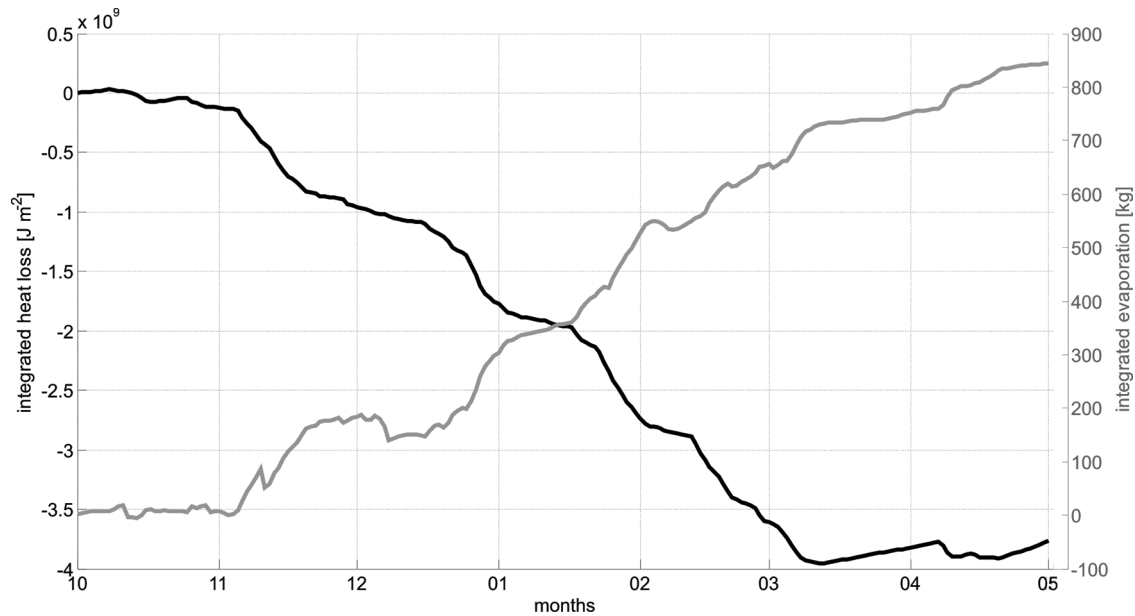


Figure 10. Integrated heat loss (black line) and net precipitation (grey line) from the ARPERA downscaling, in the period 1 October 2004 to 1 May 2005.

6.2. Surface and Lateral Heat and Salt Fluxes

[31] We now determine if the observed changes are consistent with the heat and freshwater fluxes from the daily ARPERA data set from 1 October 2004 to 1 May 2005. After extracting the integrated surface fluxes, we calculated the mean values of the lateral fluxes, resulting from (5) and (6). The impact of the different sources of error (error field associated to the MEDAR profile, and uncertainty of the atmospheric forcings) on those fluxes is assessed in section 6.3, to confirm the robustness of the results described here.

[32] The ARPERA grid point we have chosen is the closest one to station Lx in the Gulf of Lions (4.83°E, 42°N). The cumulative heat loss and net evaporation are shown in Figure 10. According to the daily ARPERA field, between October and May, the total heat loss (SHF) was $-3.77 \times 10^9 \text{ J m}^{-2}$, and the total freshwater loss was 844 mm, corresponding to a total salt gain (SSF) of 32.5 kg m^{-2} [using (4), where in this case S_{mean} is 38.44, calculated over the whole vertical profile]. Until the beginning of November, the forcings were quite weak and both the integrated heat and freshwater losses are negligible. From then on we can identify at least four periods of strong heat and freshwater losses, as shown in section 3 (Figure 6), in agreement with what *Smith et al.* [2008, Figure 15] found in the Catalan subbasin using NCEP reanalysis data.

[33] The observed heat and salt content changes (section 6.1) and the ARPERA surface fluxes allow us to estimate the

required lateral fluxes, *before* convection. Since we are considering a climatological profile, we are assuming that advection of heat and salt *during* the convection can be neglected. All the computed values are listed in Table 4 and schematized in Figure 11. Subtracting the surface fluxes from the heat and salt content changes, (5) and (6) described previously, we obtain an estimated total lateral heat advection of $3.14 \times 10^9 \text{ J m}^{-2}$ (average per unit of volume = $1.57 \times 10^6 \text{ J m}^{-3}$, with $H = 1996 \text{ m}$) and a total lateral salt advection of 33.8 kg m^{-2} (average per unit of volume = $16.9 \times 10^{-3} \text{ kg m}^{-3}$, with $H = 1996 \text{ m}$). Those values should correspond to the mean increase per unit of volume of the heat and salt contents in the advected water column. Therefore, the LHF and LSF values in Table 4 have to be considered as “anomalies” of heat and salt contents in the water advected toward the convection region. In other words, they mean that, before the convective period, the convection region has received laterally a higher amount of heat and salt than usual. In fact, from 1995 until 2004 the heat and salt contents of the water column just upstream of the convection area (represented by the DYFAMED site, Figure 7) have significantly increased. As discussed in section 4, the temporal variability of the hydrographic properties of the intermediate layer at this site provided evidence that both heat and salt contents seem to have reached maximum values during 2004, i.e., the year before the beginning of the WMT. Support to the hypothesis of a progressive heat and salt accumulation in the intermediate layer, which has

Table 4. Heat and Salt Content Changes Observed in the Water Column, Integrated Surface Fluxes From ARPERA During Winter 2004–2005, and Resulting Lateral Fluxes of Heat and Salt From Equations (3) and (4)

	Content Change (ΔHC , ΔSC)	Surface Flux (SHF, SSF)	Lateral Flux (LHF, LSF)	Anomalies at DYFAMED ^a
Heat (J m^{-2})	-0.624×10^9	-3.767×10^9	3.14×10^9 (avg. $1.57 \times 10^6 \text{ J m}^{-3}$)	0.44×10^9 (avg. $0.22 \times 10^6 \text{ J m}^{-3}$)
Salt (kg m^{-2})	66.3	32.5	33.8 (avg. $16.9 \times 10^{-3} \text{ kg m}^{-3}$)	57.0 (avg. $28.5 \times 10^{-3} \text{ kg m}^{-3}$)

^aHeat and salt content anomalies, with respect to climatology at the DYFAMED site, during fall 2004.

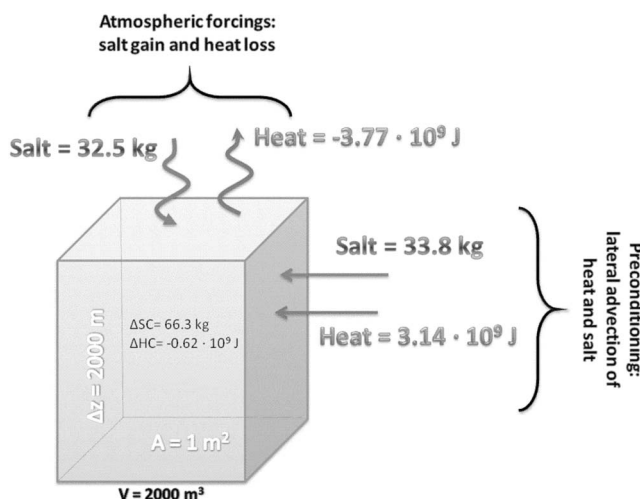


Figure 11. Scheme of the atmospheric forcings and the lateral advection acting onto a water column in the Gulf of Lions.

its origin in the EMED, is given by *Gasparini et al.* [2005, Figure 3], *Schroeder et al.* [2006, Figure 3], and *Schroeder et al.* [2009, Figure 4], showing that more salt and heat is continuously arriving from the eastern Mediterranean. The heat–salt content time series at the DYFAMED site (Figure 7) agree with this pattern.

[34] Summarizing the findings schematized in Figure 11, the large net heat loss should have induced a strong cooling of the water column ($-3.77 \times 10^9 \text{ J m}^{-2}$), which actually cooled only slightly ($-0.62 \times 10^9 \text{ J m}^{-2}$). It leads us to conclude that before the convective period a higher amount of heat was advected ($3.14 \times 10^9 \text{ J m}^{-2}$), almost compensating the loss to the atmosphere. The net evaporation during this winter, even if very high compared to the climatology for this season (section 3.2), could have induced only 49% of the actual observed increase in the salt content. This result is consistent with the long-term salinification of the intermediate layers, as hypothesized by *Schroeder et al.* [2006, 2008a]. If this is due to the propagation of the EMT from east to west, this phenomenon could have been responsible for about 51% of the observed deep salinity increase.

6.3. Uncertainties

[35] In order to test the robustness of the results, we now assess the impact of uncertainties on the resulting lateral fluxes. The effect of an increasing uncertainty in the ARPERA surface fluxes on the resulting lateral fluxes is assessed and graphically represented in Figure 12. Since the lateral fluxes are obtained by simple additions (equations (5) and (6)), their errors increase linearly with increasing surface flux errors. For instance, assuming an unlikely high uncertainty of 50% for the surface fluxes, the resulting range for the lateral heat flux becomes $3.14 \pm 1.88 \times 10^9 \text{ J m}^{-2}$ (LHF = $1.26\text{--}5.02 \times 10^9 \text{ J m}^{-2}$), while the resulting range for the lateral salt flux would be $33.8 \pm 15.5 \text{ kg m}^{-2}$ (LSF = $18.3\text{--}49.3 \text{ kg m}^{-2}$). The resulting values are still significantly positive, meaning that the lateral advection of more salt and heat toward the convection region is a robust result. Further, the range of the LSF is always positive (even with 100%

uncertainty), while the LHF becomes insignificant with surface flux uncertainties greater than 80%.

[36] The second source of error is the error field associated with the MEDAR climatology [*MEDAR Group*, 2002]. The errors to be associated to LHF and LSF are the same as the errors in the climatological heat and salt contents, and are shown in Table 3: the resulting range for the lateral heat flux is $3.14 \pm 0.313 \times 10^9 \text{ J m}^{-2}$ (LHF = $2.83\text{--}3.45 \times 10^9 \text{ J m}^{-2}$), while the resulting range for the lateral salt flux becomes $33.8 \pm 21.9 \text{ kg m}^{-2}$ (LSF = $11.9\text{--}55.7 \text{ kg m}^{-2}$). Also in this case the resulting values are still significantly positive.

[37] Comparing the effect of the two sources of errors, the resulting picture is that the climatological error field has a primary role, with regard to the lateral salt flux: the uncertainty of the surface flux would need to be at least 70% (see Figure 12b) to obtain the same effect on the error of the resulting LSF, which is an unrealistically high value. The opposite is true for heat, for which the uncertainty in the surface flux is crucial in determining error. With an error of about 8% in the surface flux (see Figure 12a) the two error sources have the same effect on the resulting LHF error.

[38] It is worth stressing that the values of LHF and LSF shown in Table 4 may be underestimated, since we are not considering the occurrence of import or export of light or dense water during the convection itself. As suggested by *Herrmann et al.* [2008], this is mainly due to mesoscale structures and the bleeding effect, i.e., the drainage of new deep water off the convection area into the boundary current flow [*Send et al.*, 1999; *Gascard*, 1978; *Visbeck et al.*, 1996].

6.4. Comparison With DYFAMED

[39] The final step in the assessment of the role of increased lateral heat and salt advection is to verify if the values of LHF and LSF computed above are realistic. For this purpose, we analyzed the DYFAMED data in order to check for consistency. As pointed out in section 6.2, the computed average heat and salt gains per unit of volume ($1.57 \times 10^6 \text{ J m}^{-3}$ and $16.9 \times 10^{-3} \text{ kg m}^{-3}$, respectively; see Table 4) are the anomalies of heat and salt contents in the water advected toward the convection region. The DYFAMED site is just upstream from the convection region (286 km between DYFAMED and station Lx), so in the following we will analyze the salt and heat contents increase over the whole water column with respect to the MEDAR climatology, to see if they can explain the required LHF and LSF estimated in section 6.2.

[40] For the following computations, we assume that the water undergoing convection in winter 2004–2005 was in the DYFAMED region in fall 2004. The anomalies of heat and salt contents in fall 2004, with respect to the MEDAR climatology in the closest grid point (43.2°N , 7.9°E), are represented in Figure 13 and listed in the last column of Table 4. The observed salt content anomaly in the Ligurian Sea (57 kg m^{-2}) would have been more than enough to explain the estimated LSF in the convection region (33.8 kg m^{-2}). On the other hand, the heat content anomaly ($0.44 \times 10^9 \text{ J m}^{-2}$) is one order of magnitude smaller than the estimated LHF ($3.14 \times 10^9 \text{ J m}^{-2}$). From the vertical distribution of the salt anomaly shown in Figure 13, an average increase of $23.3 \times 10^{-3} \text{ kg m}^{-3}$ is evident in the first 200 m, which is comparable to the LSF ($16.9 \times 10^{-3} \text{ kg m}^{-3}$).

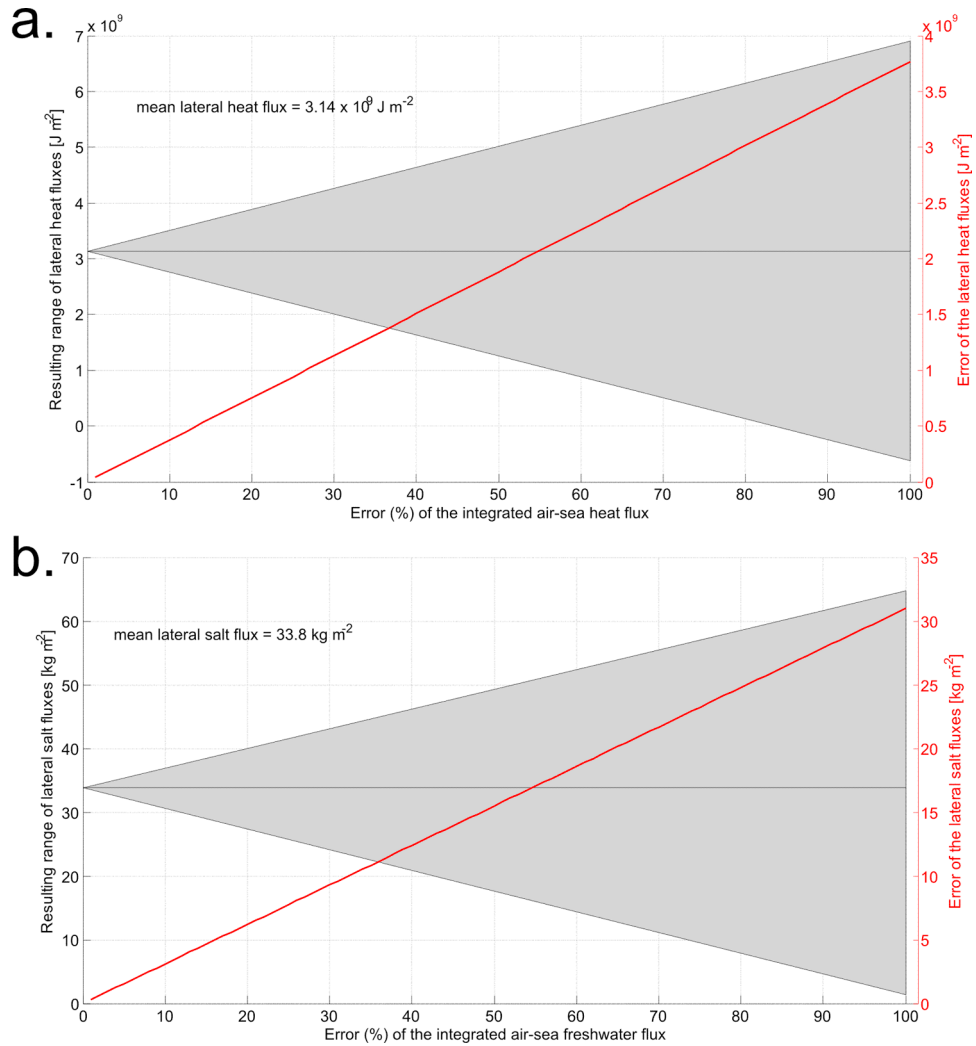


Figure 12. Effects of increasing uncertainty (%) in the surface fluxes on the resulting range of lateral fluxes (shaded area) for (above) heat and (below) salt. The red line indicates the resulting error to be associated to the mean lateral fluxes.

Nevertheless, as it was assumed by *Schroeder et al.* [2006, 2008a], the main contribution to the overall salt accumulation is due to the intermediate layer (the average anomaly of the layer 200–1200 m is $38.1 \times 10^{-3} \text{ kg m}^{-3}$, with a peak at

500–700 m), typically occupied by the LIW coming from the eastern basin. The increase in the deep layer is less pronounced and is comparable to previous estimates of the long-term trends in the WMDW [*Béthoux et al.*, 1990;

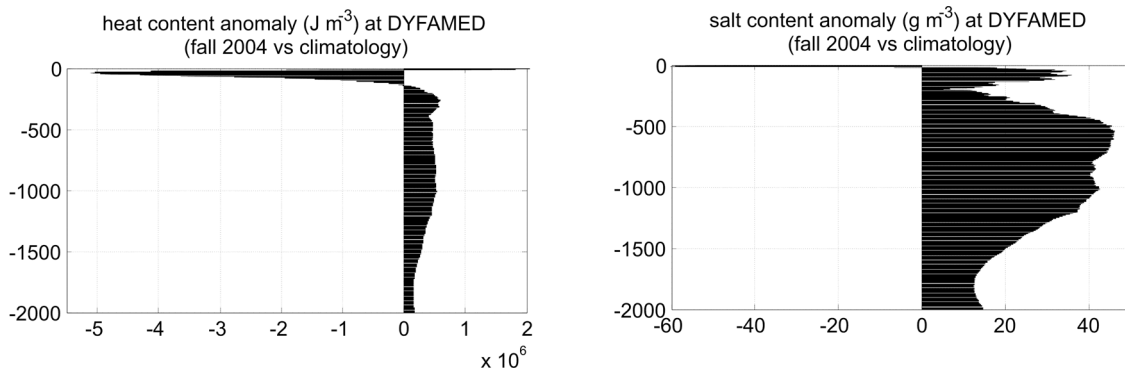


Figure 13. Vertical distribution of heat and salt content anomalies at the DYFAMED site (fall 2004 versus MEDAR climatology at 43.2°N , 7.9°E).

Béthoux and Gentili, 1999; Rixen et al., 2005; Vargas-Yanez et al., 2009]. Also in the case of heat, the main contribution comes from the lower layers, with a peak at around 300 m ($\sim 0.6 \times 10^6 \text{ J m}^{-3}$) and a negative anomaly in the first 150 m (Figure 13). However, considering the whole water column in the Ligurian Sea, the heat content per unit of volume has increased much less than the estimated LHF for the convection region in the Gulf of Lions.

[41] This comparison shows that the hypothesis of a major role of lateral salt advection in setting the new WMDW properties is consistent with observations. On the other hand, the increased heat content in the Ligurian Sea is not sufficient to explain the required lateral heat advection to the convection region. A possible explanation could be that the region has exported heat, due to mesoscale structures, during the convection itself, as shown by *Herrmann et al. [2008, Figure 5d]* and *Send et al. [1999]*. This means that the difference between the heat loss to the atmosphere and the heat content in the postwinter water column is not only due to the hydrographic preconditioning, but also to the import of warm water and the export of dense water during the event itself [*Gascard, 1978; Visbeck et al., 1996*]. A further reason might be that the strong heat loss to the atmosphere during winter 2004–2005 mainly removed the heat accumulated during summer 2004.

7. Conclusion

[42] The deep convection is sustained by the combination of surface heat and freshwater losses and the lateral convergence of heat and freshwater. The deep water properties and their variability are mainly due to the hydrographic preconditioning (heat and salt content and structure of the water column before the onset of convection), and to the atmospheric forcings (heat, freshwater and buoyancy fluxes during the convection period).

[43] During the past five years, the NW-MED seems to have become a very active DWF site. Very intense events have been reported in winter 2004–2005 as well as in winter 2005–2006, involving both open sea convection and shelf water cascading. There are other indications of DWF also in winter 2008–2009 (*J. L. Fuda, personal communication, 2009*), and its extent has to be assessed with future investigations in that region and at a basin-scale. Starting from 2005, a thermohaline anomaly is spreading throughout the western basin, filling its deeper part below 1500–2000 m depth, significantly accelerating the ventilation of the deep layers. This phenomenon has been called the Western Mediterranean Transition (WMT [*see CIESM, 2009*]).

[44] The investigation of the strength of the air-sea fluxes over recent winters, using a dynamical downscaling of the ECMWF fields and the NCEP-NCAR reanalysis, showed that winter 2004–2005 stands out as having extreme surface forcing in the Gulf of Lions region, with most of the additional heat loss due to an increase in latent heat loss. With regard to the driving meteorological terms, we found that the 2004–2005 field had a much stronger east-west pressure gradient in the WMED than in the previous winters. The reduction in air temperature combined with the strong northerly winds leads to the greater heat loss noted above. From the large-scale point of view the 2004–2005 anomaly seems to resemble the negative phase of the East Atlantic

Pattern. In both winters (2004–2005 and 2005–2006) the net evaporation, proportional to the haline term F_S , has a much weaker impact on the total density flux, than the heat loss, which drives the thermal term, F_T . This suggests that the greatly reduced precipitation in fall 2004, indicated by *Font et al. [2007]* as a possible cause of the WMT, did not play an important role in the intensity of the convection.

[45] The interannual and seasonal variability of heat and salt contents of the water column has been investigated using measurements from the DYFAMED site, used as a “proxy” for the water advected to the convection region. Although it is not a perfect proxy, at present it is the best that we can get with the available data. The general picture emerging from this analysis is as follows. There is a restratification period (April–October), characterized by a warming of the surface layer. Between October and March, the surface layer undergoes a significant cooling, which may trigger the convection in some years, together with the contribution of the increase in salt content in November–March. On the interannual time scale, there is a substantial warming and salting signal in each layer. In particular, the intermediate layers (400–1000 m) have reached the highest heat and salt contents in 2004, the year before the beginning of the WMT. After the DWF events (2004–2005 and 2005–2006), there were simultaneous salt and heat increases in the deep layer (1200–2000 m) and salt and heat decreases in the intermediate layer (400–1200 m). This evolution suggests that the increased temperature and salinity observed in the new WMDW is mainly due to internal salt and heat redistribution between intermediate and deep layers. The interannual heat and salt contents variations are the result of a combination of surface and lateral fluxes. Therefore, the lateral advection of heat and salt is computed as the difference between the heat and salt content changes and the surface fluxes. The ARPERA surface fluxes are consistent with the observed heat and salt content changes in the surface layer (0–200 m), at the DYFAMED site. The annual mean net heat loss is $-0.60 \pm 0.53 \times 10^9 \text{ J m}^{-2}$, and the annual surface freshwater loss induces a mean salt gain of $20.35 \pm 5.40 \text{ kg m}^{-2}$. The corresponding lateral fluxes, on an annual basis, were of the same order of magnitude (mean lateral heat flux = $0.70 \pm 0.52 \times 10^9 \text{ J m}^{-2}$, mean lateral salt flux = $26.98 \pm 23.65 \text{ kg m}^{-2}$). The lateral import of heat and salt comes mainly from the Tyrrhenian Sea and is advected westward along with the boundary current toward the convection region.

[46] The warmer and saltier new WMDW has firstly been formed during the exceptional winter 2004–2005, in the Gulf of Lions. The last question addressed in the paper was how the strong atmospheric forcings could have produced the thermal and haline deep anomaly. A calculation was performed to verify what would have happened if they had acted on a climatological water column. Summarizing the findings schematized in Figure 11, the large net heat loss should have induced a strong cooling of the water column ($-3.77 \times 10^9 \text{ J m}^{-2}$), which actually cooled only slightly ($-0.62 \times 10^9 \text{ J m}^{-2}$), leading us to conclude that a lateral advection of a higher amount of heat occurred ($3.14 \times 10^9 \text{ J m}^{-2}$), almost compensating for the loss to the atmosphere. The net evaporation during this winter, even if very high compared to the climatology for this season, could have induced only 49% of the actual observed increase in the salt

content. This result is consistent with the long-term salinification of the intermediate layers, as hypothesized by Schroeder et al. [2006, 2008a]. A similar scenario has been shown by Boscolo and Bryden [2001] for Aegean Sea deep water formation in the early 1990s, where the effective increase in net evaporation slowly increases the salinity and decreases the stratification in the Aegean Sea until a severe winter leads to deep convection and new bottom water formation. The assessments of the different sources of errors in the calculation and the comparison with observations at the DYFAMED site have shown that the lateral advection of more salt toward the convection region is a robust result. In the case of heat, the increased heat content in the Ligurian Sea is not sufficient to explain the required lateral heat advection to the convection region, suggesting that the difference between the heat loss to the atmosphere and the heat content change is not only due to hydrographic preconditioning, but also to the import of warm water and the export of dense water during the event itself.

[47] The paper also shows that the WMDW formed during the non-exceptional winter 2005–2006 was characterized by anomalously high heat and salt contents, suggesting a major role of the hydrographic preconditioning in setting the new deep water properties, with respect to atmospheric forcings. Grignon et al. [2010] studied the relative importance of the variability of the surface forcing and preconditioning on the composition of the water formed. They found that the resulting salinity of the water formed is mainly set by the initial salt content of the water content, with no or very little impact of the surface freshwater fluxes, whereas the temperature of the deep water formed is affected by both the initial heat content and the surface heat fluxes. Wu and Haines [1996] pointed out that an increase of the subsurface salinity maximum in the NW-MED is able either to increase the depth of the convection or to affect the temperature and salinity properties of the new water. From this point of view, air-sea interaction would remain the principal driving force of the Mediterranean circulation, but the occurrence of extreme events would depend on the contemporary presence of the appropriate oceanic conditions [Artale et al., 2006].

[48] This study has evidenced that, despite several advances in the recent years, there are still huge gaps in current knowledge, as well as a need for further monitoring, of these temperature and salinity anomalies (including physical, biological, chemical and sedimentological parameters, see CIESM [2009]). Further investigations should also attempt to explain the cause of the observed increasing temperature and salinity of the intermediate water crossing the Sicily Channel. Further, as suggested by Millot [2007], the interannual variability of the inflow through Gibraltar, in particular the observed increasing salt content of the inflowing AW, should be taken into account.

[49] **Acknowledgments.** The authors acknowledge the Observatoire Océanologique de Villefranche sur Mer Service d'Observation and, in particular, Laurent Coppola for providing the DYFAMED monthly CTD time series. The NCEP-NCAR fields were obtained from the International Research Institute for Climate Prediction/Lamont-Doherty Earth Observatory Climate Data Library (<http://ingrid.ligo.columbia.edu>). This research has been supported by the MEDCLIVAR Programme (grant 1944). Finally, the authors are grateful for the comments of Manuel Vargas-Yanez and an anonymous reviewer that contributed to improving the manuscript.

References

- Alberola, C., C. Millot, and J. Font (1995), On the seasonal and mesoscale variabilities of the Northern current during the PRIMO 0 experiment in the western Mediterranean Sea, *Oceanol. Acta*, *18*, 163–192.
- Artale, V., S. Calmanti, P. Malanotte-Rizzoli, G. Pisacane, V. Rupolo, and M. Tsimplis (2006), The Atlantic and the Mediterranean Sea as connected systems, in *Mediterranean Climate Variability*, edited by P. Lionello, P. Malanotte-Rizzoli, and R. Boscolo, pp. 283–323, Elsevier, Amsterdam, Netherlands.
- Béthoux, J., and B. Gentili (1999), Functioning of the Mediterranean Sea: Past and present changes related to freshwater input and climate changes, *J. Mar. Syst.*, *20*, 33–47.
- Béthoux, J., B. Gentili, J. Raunet, and D. Tailliez (1990), Warming trend in the western Mediterranean deep water, *Nature*, *347*, 660–662.
- Bindoff, N. L., and T. J. McDougall (1994), Diagnosing climate change and ocean ventilation using hydrographic data, *J. Phys. Oceanogr.*, *24*, 1137–1152.
- Boscolo, R., and H. L. Bryden (2001), Causes of long-term changes in Aegean sea deep water, *Oceanol. Acta*, *24*(6), 519–527.
- Commission Internationale pour l'Exploration Scientifique de la mer Méditerranée (CIESM) (2009), *Dynamics of Mediterranean Deep Waters*, CIESM Workshop Monogr., vol. 38, edited by F. Briand, 132 pp., CIESM, Monaco.
- Déqué, M., and J. Piedelievre (1995), High-resolution climate simulation over Europe, *Clim. Dyn.*, *11*, 321–339.
- Font, J., P. Puig, J. Salat, A. Palanques, and M. Emelianov (2007), Sequence of hydrographic changes in NW Mediterranean deep water due to the exceptional winter of 2005, *Sci. Mar.*, *71*(2), 339–346.
- Gascard, J. C. (1978), Mediterranean deep water formation, baroclinic instability and oceanic eddies, *Oceanol. Acta*, *1*, 315–330.
- Gasparini, G. P., A. Ortona, G. Budillon, M. Astraldi, and E. Sansone (2005), The effect of the Eastern Mediterranean Transient on the hydrographic characteristics in the Strait of Sicily and in the Tyrrhenian Sea, *Deep Sea Res., Part I*, *52*(6), 915–935.
- Gasparini, G. P., K. Schroeder, and S. Sparnocchia (2008), Straits and channels as key regions of an integrated marine observatory of the Mediterranean: Our experience on their long-term monitoring, in *Towards Integrated Mediterranean Marine Observatories*, CIESM Workshop Monogr., vol. 34, pp. 75–79, CIESM, La Spezia, Italy.
- Gill, A. E. (1982), *Atmosphere-Ocean Dynamics*, Int. Geophys. Ser., vol. 30, 662 pp., Academic Press, San Diego, Calif.
- Grignon, L., D. Smeed, H. L. Bryden, and K. Schroeder (2010), Importance of the variability of hydrographic preconditioning for deep convection in the Gulf of Lion, NW Mediterranean, *Ocean Sci. Discuss.*, *6*, 1–40.
- Herrmann, M., and S. Somot (2008), Relevance of ERA40 dynamical downscaling for modeling deep convection in the North-Western Mediterranean Sea, *Geophys. Res. Lett.*, *35*, L04607, doi:10.1029/2007GL032442.
- Herrmann, M., S. Somot, F. Sevault, C. Estournel, and M. Déqué (2008), Modelling the deep convection in the north-western Mediterranean Sea using an eddy-permitting and an eddy-resolving model: Case study of winter 1986–1987, *J. Geophys. Res.*, *113*, C04011, doi:10.1029/2006JC003991.
- Josey, S. A. (2003), Changes in the heat and freshwater forcing of the eastern Mediterranean and their influence on deep water formation, *J. Geophys. Res.*, *108*(C7), 3237, doi:10.1029/2003JC001778.
- Josey, S. A., and R. Marsh (2005), Surface freshwater flux variability and recent freshening of the North Atlantic in the Eastern Subpolar Gyre, *J. Geophys. Res.*, *110*, C05008, doi:10.1029/2004JC002521.
- Josey, S. A., E. C. Kent, and B. Sinha (2001), Can a state of the art atmospheric general circulation model reproduce recent NAO related variability at the air-sea interface? *Geophys. Res. Lett.*, *28*(24), 4543–4546, doi:10.1029/2001GL013200.
- Kistler, R., et al. (2001), The NCEP-NCAR 50-year reanalysis: Monthly means CD-ROM and documentation, *Bull. Amer. Meteorol. Soc.*, *82*, 247–267.
- Klink, J. M. (1998), Heat and salt changes on the continental shelf west of the Antarctic Peninsula between January 1993 and January 1994, *J. Geophys. Res.*, *103*, 7617–7636, doi:10.1029/98JC00369.
- Li, L., A. Bozec, S. Somot, K. Béranger, P. Bouruet-Aubertot, F. Sevault, and M. Crépon (2006), Regional atmospheric, marine processes and climate modeling, in *Mediterranean Climate Variability*, edited by P. Lionello, P. Malanotte-Rizzoli, and R. Boscolo, pp. 373–398, Elsevier, Amsterdam, Netherlands.
- Lopez-Jurado, J., C. Gonzalez-Pola, and P. Velez-Belchi (2005), Observation of an abrupt disruption of the longterm warming trend at the Balearic Sea, western Mediterranean sea, in summer 2005, *Geophys. Res. Lett.*, *32*, L24606, doi:10.1029/2005GL024430.
- MEDAR Group (2002), *Mediterranean and Black Sea Database of Temperature, Salinity and Biochemical Parameters and Climatological Atlas*

- [CD-ROM], Inst. Fr. de Rech. pour l'Exploit. de la Mer, Plouzane, France.
- MEDOC Group (1970), Observation of formation of deep water in the Mediterranean Sea, 1969, *Nature*, 227, 1037–1040.
- Millot, C., and I. Taupier-Letage (2005), Circulation in the Mediterranean Sea, in *The Mediterranean Sea, The Handbook of Environmental Chemistry*, vol. 5K, pp. 29–66, Springer, Berlin.
- Millot, C. (2007), Interannual salinification of the Mediterranean inflow, *Geophys. Res. Lett.*, 34, L21609, doi:10.1029/2007GL031179.
- Rhein, M. (1995), Deep water formation in the western Mediterranean, *J. Geophys. Res.*, 100(C4), 6943–6959, doi:10.1029/94JC03198.
- Rixen, M., et al. (2005), The Western Mediterranean deep water: A proxy for climate change, *Geophys. Res. Lett.*, 32, L12608, doi:10.1029/2005GL022702.
- Roether, W., B. Klein, B. B. Manca, A. Theocharis, and S. Kioroglou (2007), Transient Eastern Mediterranean deep waters in response to the massive dense-water output of the Aegean Sea in the 1990s, *Prog. Oceanogr.*, 74, 540–571.
- Rogers, J. C. (1990), Patterns of low-frequency monthly sea level pressure variability (1899–1986) and associated wave cyclone frequencies, *J. Clim.*, 3, 1364–1379.
- Salat, J., and J. Font (1987), Water mass structure near and offshore the Catalan coast during the winters of 1982 and 1983, *Ann. Geophys.*, 1B, 49–54.
- Samuel, S. L., K. Haines, S. A. Josey, and P. G. Myers (1999), Response of the Mediterranean Sea thermohaline circulation to observed changes in the winter wind stress field in the period 1980–93, *J. Geophys. Res.*, 104(C4), 7771–7784, doi:10.1029/1998JC900130.
- Schmitt, R. W., P. S. Bogden, and C. E. Dorman (1989), Evaporation minus precipitation and density fluxes for the North Atlantic, *J. Phys. Oceanogr.*, 19: 1208–1221.
- Schroeder, K., G. P. Gasparini, M. Tangherlini, and M. Astraldi (2006), Deep and intermediate water in the Western Mediterranean under the influence of the Eastern Mediterranean Transient, *Geophys. Res. Lett.*, 33, L21607, doi:10.1029/2006GL027121.
- Schroeder, K., A. Ribotti, M. Borghini, R. Sorgente, A. Perilli, and G. P. Gasparini (2008a), An extensive western Mediterranean deep water renewal between 2004 and 2006, *Geophys. Res. Lett.*, 35, L18605, doi:10.1029/2008GL035146.
- Schroeder, K., M. Borghini, G. Cerrati, V. Difesca, R. Delfanti, C. Santinelli, and G. P. Gasparini (2008b), Multiparametric mixing analysis of the deep waters in the western Mediterranean Sea, *Chem. Ecol.*, 24(1), 47–56.
- Schroeder, K., V. Taillandier, A. Vetrano, and G. P. Gasparini (2008c), The circulation of the western Mediterranean Sea in spring 2005 as inferred from observations and from model outputs, *Deep Sea Res. Part I*, 55, 947–965.
- Schroeder, K., G. P. Gasparini, M. Borghini, and A. Ribotti (2009), Experimental evidences of the recent abrupt changes in the deep Western Mediterranean Sea, in *Dynamics of Mediterranean deep water*, CIESM Workshop Monographs, vol. 38, pp. 51–56, edited by F. Briand, CIESM, Monaco.
- Send, U., J. Font, G. Krahnmann, C. Millot, M. Rhein, and J. Tintoré (1999), Recent advances in observing the physical oceanography of the western Mediterranean Sea, *Prog. Oceanogr.*, 44, 37–64.
- Simmons, A., and J. Gibson (2000), The ERA-40 project plan, in *ERA-40 project report series Tech. Rep. 1*, edited by ECMWF, Shinfield Park, Reading, UK.
- Smith, R. O., H. L. Bryden, and K. Stansfield (2008), Observations of new western Mediterranean deep water formation using ARGO floats 2004–2006, *Ocean Sci.*, 4, 133–149.
- Sparnocchia, S., P. Picco, G. M. R. Manzella, A. Ribotti, S. Copello, and P. Brasey (1995), Intermediate water formation in the Ligurian Sea, *Oceanol. Acta*, 12, 151–162.
- Straneo, F. (2006), Heat and freshwater transport through the central Labrador Sea, *Journal of Phys. Oceanogr.*, 36, 606–628.
- Vargas-Yanez, M., P. Zunino, A. Benali, M. Delpy, F. Pastre, F. Moya, M. C. Garcia-Martinez, and E. Tel (2009), How much is the Western Mediterranean really warming and salting? *J. Geophys. Res.*, 115, C04001, doi:10.1029/2009JC005816.
- Visbeck, M., J. Marshall, and H. Jones (1996), Dynamics of isolated convective regions in the ocean, *J. Phys. Oceanogr.*, 26, 1721–1734.
- Wu, P., and K. Haines (1996), Modeling the dispersal of Levantine Intermediate Water and its role in Mediterranean deep water formation, *J. Geophys. Res.*, 101(C3), 6591–6607, doi:10.1029/95JC03555.

H. L. Bryden, L. Grignon, and S. A. Josey, National Oceanography Centre, Southampton, University of Southampton Waterfront Campus, European Way, Southampton, SO14 3ZH, UK. (H.Bryden@noc.soton.ac.uk; laure.grignon@noc.soton.ac.uk; S.A.Josey@soton.ac.uk)

M. Herrmann, Météo-France/CNRM, 42 avenue Gaspard Coriolis, 31057 Toulouse Cedex 1, France. (marine.herrmann@cnrm.meteo.fr)

K. Schroeder and G. P. Gasparini, CNR-ISMAR/Sede di La Spezia, Forte Santa Teresa, 19036 Pozzuolo di Lerici, Italy. (Katrin.schroeder@ismar.cnr.it; gasparini@sp.ismar.cnr.it)